

Fibonacci structure in conch shell

The conch shell has been used by various cultures on diverse occasions through the ages. Particularly in India it has been described in the puranas and epics and is being used almost in all Indian societies during auspicious occasions. However, the conch shell as a musical instrument has not been investigated as yet. Bhat and coworkers¹⁻⁴ have reported the X-ray tomographic picture and the conch sound spectrum in recent past only.

In order to study the acoustics of the conch shell, the study of its structure is important. Here, we present the results of an investigation on this aspect. Figure 1 *a-c* shows the X-ray tomograph of conch shells and a photograph of a dissected shell. It can be seen that the structure grows in spiral both in the transverse and longitudinal directions. Our measurement of the parameters in the structure satisfy the celebrated Fibonacci patterns found abundantly in nature^{5,6}. The parameters, when judiciously chosen, fairly furnish the Fibonacci pattern and golden ratio.

Next we outline the Fibonacci sequence, its occurrence in nature, the Fibonacci

rectangle and spirals. Finally, we present the Fibonacci pattern in conch shells.

The number sequence generated by the rule $f_1 = f_2 = 1$, $f_{N+1} = f_N + f_{N-1}$ is named after the celebrated European mathematician, Fibonacci (AD 1170–1240), and turns out to be 1, 1, 2, 3, 5, 8, 13, 21, 34, 55, 89, 144, 233, 377, 610, 987, The ratio of the successive pairs tends to the well-known golden ratio Φ (F_N/F_{N-1}) = 1.618033989. It is interesting to note that $\Phi^{-1} = 0.618033989$, so that $1/\Phi = \Phi - 1$, which is reckoned magic.

The Fibonacci method is best suited when the interval containing the minimum of the interval of uncertainty is to be reduced to a given value in the least number of trials. This can be interpreted as maximum reduction of the interval of uncertainty in the given number of trials.

Maximum reduction of interval of uncertainty is given by

$$I_2 = \frac{F_N}{F_{N+1}} I_1.$$

Using $I_3 = I_1 - I_2$, new intervals can be generated, where $F_N/F_{N+1} = 0.61803 = (\sqrt{5}-1)/2$ or $F_{N+1}/F_N = 1.61803$ and

$$(F_N/F_{N+1})^2 + (F_N/F_{N+1}) - 1 = 0.$$

Hence the ratio

$$F_N/F_{N+1} = \frac{\sqrt{5}-1}{2} \text{ or } \frac{-(\sqrt{5}+1)}{2}.$$

The ratio $360/222.49 = 1.618$ and hence 222.49° or its supplement 137.51° are taken as golden angles. This sequence is recognized as the divine sequence of nature. The Fibonacci sequence is utilized not only as a number system, but also as a series of rectangles and spirals generated out of the rectangles, a form which occurs in nature in a number of instances.

A brief outline of the process of drawing the rectangles and thereby spirals is as follows. Start with two, unit squares drawn side by side. Then a new square of side two units is drawn touching both the unit squares. The fourth square is drawn

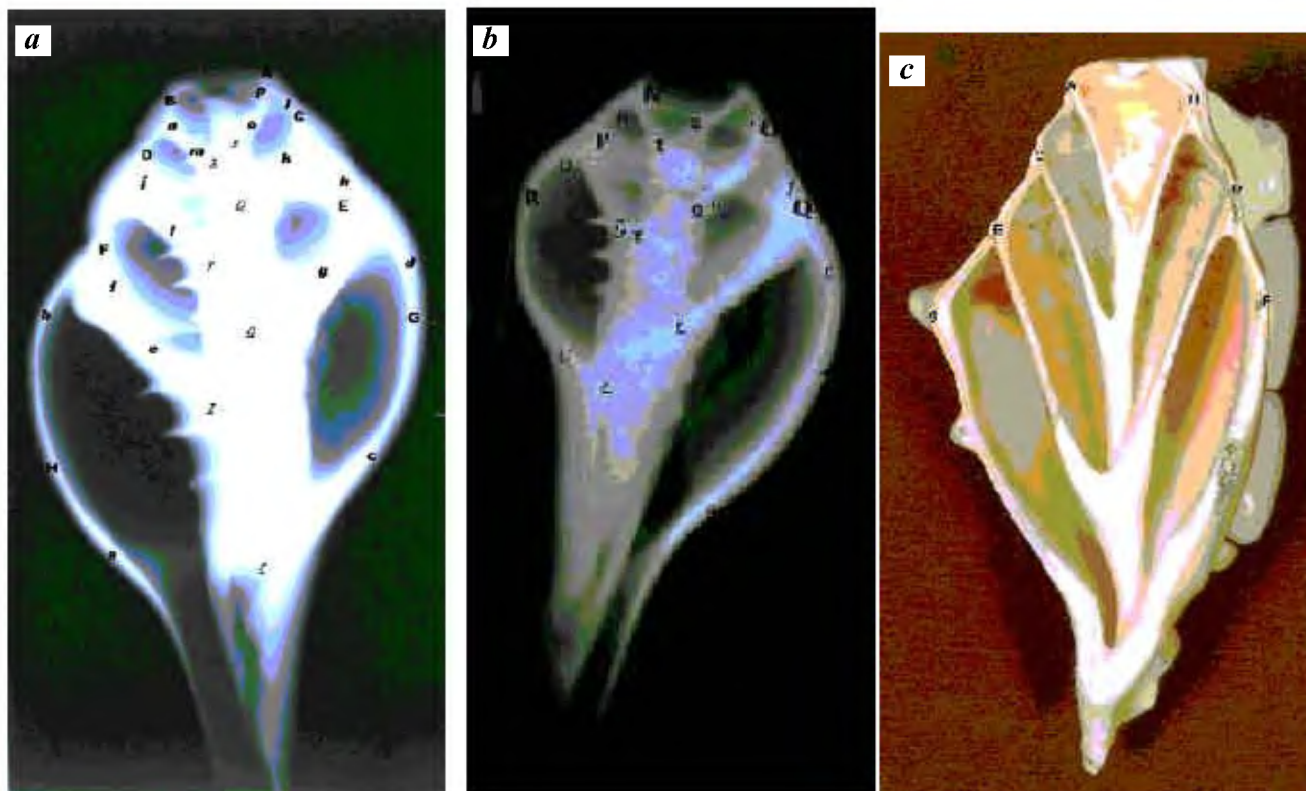


Figure 1. *a, b*, X-ray tomograph of a conch shell. *c*, Photograph of a dissected conch shell.

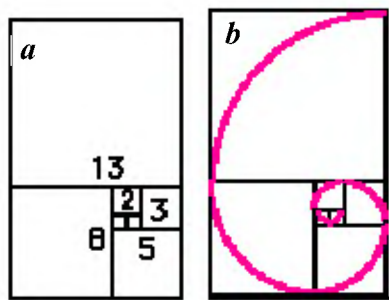


Figure 2. *a*, Fibonacci rectangle. *b*, Spiral constructed through the fibonacci rectangle.

Table 1. Labelled parameters on transverse and longitudinal growth of conch shell (shown in Figure 1 *a*). The ratio of consecutive figures falls close to the golden ratio

AB (D_1)	02 cm
CD (D_2)	03 cm
EF (D_3)	05 cm
GH (D_4)	08 cm
BC (R_1)	2.5 cm
DE (R_2)	4 cm
FG (R_3)	6.4 cm
<i>sp</i>	1.6 cm
<i>pq</i>	2.6 cm
<i>qr</i>	4.3 cm
<i>xy</i>	2 cm
<i>yz</i>	3.1 cm

Table 2. Values of labelled parameters in the second sample (shown in Figure 1 *b*)

NO (D_2)	1.5 cm
PQ (D_3)	2.5 cm
RS (D_4)	3.5 cm
OP (R_1)	2.0 cm
QR (R_2)	3.2 cm
<i>xy</i>	1.2 cm
<i>yz</i>	0.2 cm
<i>pq</i>	1.0 cm
<i>qr</i>	1.6 cm

Table 3. Values of labelled parameters from dissected conch sample (shown in Figure 1 *c*)

AB	2.0 cm
CD	3.2 cm
EF	5.0 cm
BC	2.5 cm
DE	4.0 cm
FG	6.0 cm

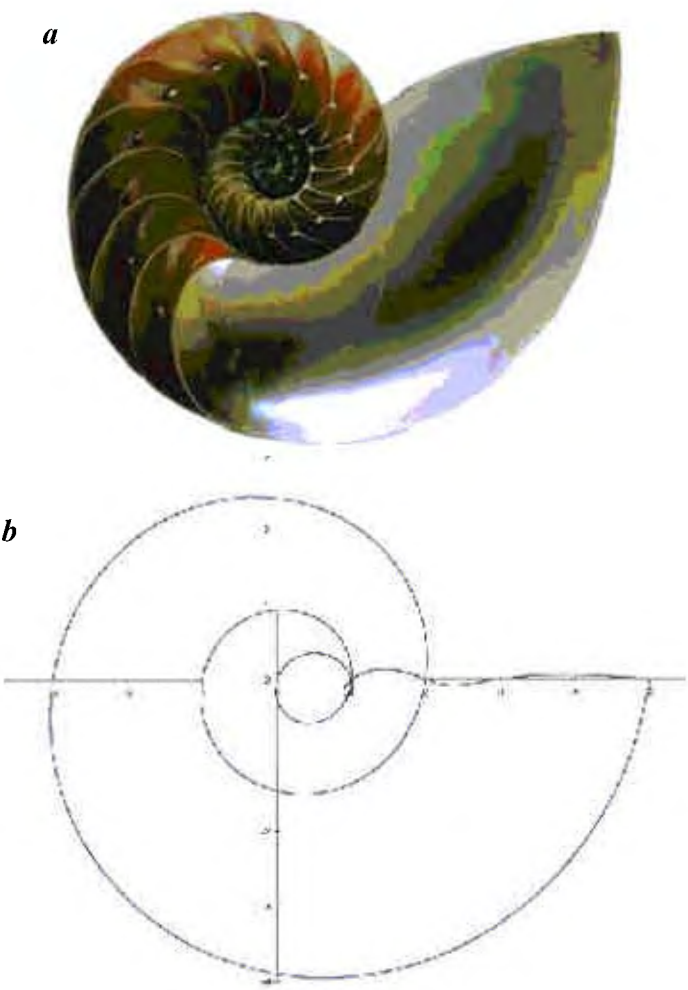


Figure 3. *a*, Spiral structure of a nautilus shell. *b*, Curve crossing the X-axis at the Fibonacci numbers.

with side three units, touching on any one side, the first and the third squares. The process is successively repeated on the sides with lengths equal to the sum of two immediate preceding squares, while maintaining a definite sense of rotation. The process is demonstrated in Figure 2 *a*. This set of rectangles whose sides are two successive Fibonacci numbers, is the Fibonacci rectangle. To draw the spiral, a semi-circle is first drawn inside the first two squares with the sum of two unit sides as diameter. The circle is extended by drawing another quarter circle inside the third square, by joining the end of first semi circle and the opposite corner of the third square with a radius equal to the length of the side of the square. The process is repeated with a definite sense of rotation, each time by drawing a quarter circle inside successive squares with radius equal to the edge of each respective side. A smooth spiral thus comes out (Figure 2 *b*).

Obviously, the Fibonacci rectangles involve the golden ratio and the spiral also expands in the same ratio. This spiral is similar to that found in the shell of certain molluscs, including snails and nautilus shells (Figure 3 *a*). Figure 3 *b* is an equiangular spiral, generated on a computer, which exactly fits the snail spiral. Hence the Fibonacci spiral may be taken as equiangular spiral. It will not be out of place to mention here that Fibonacci patterns are found in plant growth, leaf patterns, floral petals and stems. Fibonacci helix can be seen in pine cone, pineapple and teazles; the golden ratio is found in the human body, and art and architecture through the ages⁵⁻⁷.

The X-ray tomographic pictures of conch shells (Figure 1 *a* and *b*) may be matched with an enlarged version of Figure 3 *b* to give exact piece-wise matching in the longitudinal growth. But morphological structure of the conch shell is different

from a snail shell. The snail shell is approximately a two-dimensional spiral. In case of the conch shell, the spiral coils around a central axis called the columella or central pillar of the shell. Figure 1 *a–c* clearly shows that the cavity around the central pillar grows both in the horizontal and vertical directions. Results of measurement of longitudinal and transverse cavity dimensions according to labels in Figure 1 *a–c* are shown in Tables 1–3 respectively. It may be noticed that the ratios of selectively taken parameters fall fairly close to the golden value.

The golden ratios are nearly borne out in all the tested samples. It has also been checked by matching the X-ray tomographs with the computer-generated spiral that the curves *ab*, *cd*, *ef*, *gh*, *ij*, *kl*, *mn* in Figure 1 *a* and *b* exactly fit with appropriate sections of the spiral.

We have shown that the spiral structure of the conch shell clearly exhibits Fibonacci pattern. Our study has been limited

to a few samples of conch shells. But in view of the symmetry of conch structure, we deem the findings to be a generalization. However, deviation might be possible in certain conch species.

1. Bhat, R. B., Proceedings of the National Seminar of Acoustics and its Biological Effects, Chennai, 20–22 December 1985.
2. Bhat, R. B., *J. Sound Vib.*, 1992, **157**, 190–191.
3. Bhat, R. B., Proceedings of the National Symposium on Acoustics, 12–15 December 1992.
4. Taylor, L. R., Prasad, M. G. and Bhat, R. B., Proceedings of the 3rd International Congress on Air and Structure-borne Sound and Vibration, 13–15 June 1994, Montreal, pp. 1695–1701.
5. Ghyka, Matila, *The Geometry of Art and Life*, Dover, 1978, pp. 87–210.
6. Fibonacci number in nature, science mysteries; World-mysteries.com
7. Cook, T. A., *The Curves of Life*, Dover, 1979.

ACKNOWLEDGEMENTS. We thank B. K. Samal and A. Singh, Nehru Satabdi Central Hospital, Talcher for their cooperation in taking the X-ray tomography of conch shell samples. We also thank M. K. Pani, Kaniha, Talcher for digital conversion of X-ray and the still photographs.

Received 2 January 2004; revised accepted 23 November 2004

SAROJ KUMAR RATH^{1,*}
P. C. NAIK²

¹*Department of Physics,
Talcher College,
Talcher 759 107, India*

²*Department of Physics,
D. D. College,
Keonjhar 758 001, India*

*For correspondence.
e-mail: sarojkarath@yahoo.co.in

Ductile shearing along the Great Boundary Fault: An example from the Berach river section, Chittaurgarh, Rajasthan

The Great Boundary Fault manifests itself as a northeast striking tectonic lineament that cuts the Precambrian crust in Rajasthan for strike length of more than 400 km. Geophysical studies indicate that this fault continues under the Gangetic alluvium¹, dips at a steep angle towards northwest and cuts a thick section of the crust up to a near Moho depth^{2–4}. That the Great Boundary Fault has developed as a consequence of brittle style of deformation is well entrenched in geological literature since the pioneering contributions^{5–11}. There has, however, been considerable controversy regarding the initiation and reactivation of this fault, i.e. normal to reverse¹², or, thrust to normal¹³. Palaeostress analyses reveal that the tectonic evolutionary history of the Great Boundary Fault records three distinct phases of reactivation, each typified by a characteristic style of brittle faulting¹⁴. A recent study indicates the ductile nature of deformation in the Upper Vindhyan and the Ranthambore Groups of rocks, exposed in the vicinity of the Great Boundary Fault¹⁵. Here we report the occurrence of mylonites in the Lower

Vindhyan rocks, and demonstrate that ductile shearing, responsible for the development of these mylonites, is the earliest event of tectonic deformation within the Great Boundary Fault zone.

Two distinct types of deformation zones¹⁵ can be identified within the study area (Figure 1 *a*). First, an approximately 150 m wide fault zone, namely the Great Boundary Fault Zone GBFZ, which is characterized by the occurrence of numerous metre-scale ductile shear zones, two groups of successively developed mesoscopic folds, F_1 and F_2 and the intense nature of F_2 folding. Second, an approximately 5 km wide fault-related deformation zone, which consists of metre-scale brittle faults and en-echelon veins that cut through kilometre-scale F_2 folds¹⁴. In the fault-related deformation zone, F_1 folds and ductile shear zones are characteristically lacking, and F_2 folding is distinctly less intense than the F_2 folding in the fault zone. Here we focus on the nature of deformation within the GBFZ, which cuts through the Nimbahera shale beds exposed in the Berach river section (Figure 1 *a*). The nature of deformation

within the fault-related deformation zone has been described elsewhere¹⁴.

It is noteworthy that the GBFZ in the Berach river section cuts through the Vindhyan rocks rather than following the contact between the Berach granite and the Vindhyan sedimentary rocks^{11,12} (Figure 1 *a*). The outcrop pattern within the GBFZ is controlled by characteristically open to gentle and upright F_2 folds that plunge at low angles towards NE and/or SW (Figure 1 *b* and *c*). Many of these folds define periclinal domes and basins, and the individual fold hinge lines commonly bifurcate at moderate angles (*c.* 45°). Several lines of evidence, such as the direct relationship between thickness of beds and wavelength of folds, the branching of hinge lines, the reversal in sense of shear offset at the opposite limbs, and the orthogonal relationship between the hinge lines and striations on the fold limbs imply that these folds were developed by flexural slip mechanism due to layer parallel compression.

Ductile shear zones, the other major characteristic structure of the GBFZ in the Berach river section, occur as metre-scale